Plasmonics (2010) 5:251–258
DOI 10.1007/s11468-010-9145-8

# Achieving Invisibility of Homogeneous Cylindrically Anisotropic Cylinders

**Yaxian Ni · Lei Gao · Cheng-Wei Qiu**

Received: 26 January 2010 / Accepted: 6 May 2010 / Published online: 22 May 2010


**Abstract** In this paper, we establish the full-wave electromagnetic scattering theory to study the electromagnetic scattering from infinitely long cylinders with cylindrically anisotropic coatings. We show that the total effective scattering width can be dramatically reduced by the suitable adjustment of the dielectric anisotropy of the shell, while it is not the case for tuning the dielectric anisotropy of the core. Furthermore, we could make the cylindrical objects invisible when both dielectric and magnetic anisotropies are adjusted. In the long wavelength limit, we develop effective medium theory to derive the effective isotropic permittivity and permeability for the anisotropic coated cylinders, and the invisibility radius ratio derived from the full-wave theory for small coated cylinders can be well described within the effective medium theory.

**Keywords** Electromagnetic scattering · Cylindrical anisotropy · Effective medium theory · Coated cylinder · Invisibility

Y. Ni · L. Gao
Jiangsu Key Laboratory of Thin Films,
Department of Physics, Soochow University,
Suzhou 215006, China

L. Gao
e-mail: leigao@suda.edu.cn

C.-W. Qiu (✉)
Department of Electrical and Computer Engineering,
National University of Singapore, 4 Engineering Drive 3,
Singapore 117576, Singapore
e-mail: eleqc@nus.edu.sg

## Introduction

In recent years, designing optical and electromagnetic (EM) invisibility cloaking devices has attracted great attention from both physics and engineering societies. Scientists have developed coordinate transformation method [1] and conformal mapping method [2], which can protect the cloaked object of arbitrary shape from electromagnetic radiation. This idea has been verified by full-wave simulation of the cylindrical cloaking structure based on both finite element method [3] and finite-difference time-domain method [4]. The experimental demonstration at microwave frequencies [5] and even at optical frequencies [6] for non-magnetic material has been realized lately. They have investigated the transformation-based cloaks possessing spherical/cylindrical geometries with rotational symmetry [1, 5, 7–9] and geometries with reduced symmetries, such as eccentric elliptic cylinders [10], square cloaks [11], and arbitrary shapes [12]. In addition to the method of spatial transformation, Alu et al. have proposed to use isotropic plasmonic coatings to render objects invisible [13] based on the dipolar cancellation and proposed a parallel-plate metamaterial cloak [14] that significantly reduces the total scattering cross section of a given two-dimensional dielectric obstacle in some frequency band.

Due to the spatial compression, the required parameters should be anisotropic and dependent on the position [1]. To alleviate these constraints, EM invisibility cloaks have been realized by isotropic coatings based on the effective medium theory [15, 16]. However, it still requires sufficient layers of alternating isotropic media in order to maintain the validity of the effective medium theory. Although recent development in

metamaterial may allow the control of material parameters, such strict requirements for the parameters of a perfect cloak are still too difficult to realize in practice. As a way to reduce the number of required constitutive parameters to realize a manufacturable cloak, the incidence can be decomposed into transverse electric (TE) and transverse magnetic (TM) components so that 2D cloaks with simplified parameters [17, 18] can be used. Unfortunately, the simplified cylindrical cloak will cause large reflection at the cloak's outer boundary due to the impedance mismatch. From the discussion above, one can see that (1) ideal cylindrical cloaks require six parameters, some of which are infinite values; (2) simplified cylindrical cloaks requires three parameters but still some value tends to the infinity at the inner boundary; and (3) both ideal and simplified cylindrical cloaks need certain parameters to be inhomogeneous, i.e., a function of position. This motivates our current work on achieving cylindrical cloaks, which is based on only one single coating by a homogeneous and cylindrically anisotropic medium. The invisibility condition can be established by the effective medium theory. It is obvious that the constraints in material fabrication are greatly alleviated.

A lot of theoretical and numerical approaches have been developed to deal with the scattering problem of homogeneous anisotropic or even gyrotropic cylinders, e.g., integrodifferential equation [19, 20], volumetric integral equation method [21], combined field surface integral equation method [22], finite difference method with measured equation of invariance [21], and dyadic Green's functions [23–25]. However, it should be noted that all these anisotropic tensors in those mentioned papers are defined in Cartesian coordinates, which is different from the cylindrically anisotropy defined in the cylindrical coordinates as discussed in this paper. Although the latter can be mapped into Cartesian anisotropy, then the anisotropic cylinder will be inhomogeneous and angle dependent.

Following our discussed motivation, in order to investigate the EM invisibility of cylindrically anisotropic coated cylinders, we develop the compact scattering theorem for a coated cylinder with homogeneous cylindrical anisotropy, by extending the idea of embedding cylindrical anisotropy in the orders of Bessel/Hankel functions in spherical case [26]. We focus our analysis on the invisibility characteristics of a homogeneous anisotropic coated cylinder. EM field components and scattering width of such coated cylinders are formulated. We discuss the roles of anisotropic parameters as well as the core–shell ratio on the reduction of the total scattering section. From the scattering algorithm, the effective permeability and permittivity of the core–shell system are also established so that the required condition for invisibility performance can be exactly determined. The numerical results are given. This method provides a promising alternative way to tailor the plasmonics of nanorods [27, 28] with a special anisotropy to achieve the invisibility with less demanding requirements on parameters.

## Full-wave electromagnetic scattering theory

Let us consider the electromagnetic scattering from a cylindrically anisotropic coated cylinder of infinite length (see Fig. 1). For the simplicity, we assume a normally incident plane wave with the magnetic field along the $z$ direction (i.e., the TM wave). We assume that the coated cylinder is composed of the core with the radius $a$ and the shell with the radius $b$, and it is surrounded by free space $(\varepsilon_0, \mu_0)$. As for cylindrical anisotropy, we indicate that the permeability and the permittivity tensors for the core and the shell can be expressed in cylindrical coordinates $(\hat{r}, \hat{\theta}, \hat{z})$,

$$\overline{\overline{\varepsilon}}_p = \begin{pmatrix} \varepsilon_{pr} & 0 & 0 \\ 0 & \varepsilon_{p\theta} & 0 \\ 0 & 0 & \varepsilon_{pz} \end{pmatrix} \tag{1a}$$

$$\overline{\overline{\mu}}_p = \begin{pmatrix} \mu_{pr} & 0 & 0 \\ 0 & \mu_{p\theta} & 0 \\ 0 & 0 & \mu_{pz} \end{pmatrix}, \tag{1b}$$

where $\overline{\overline{\varepsilon}}_p$ (or $\overline{\overline{\mu}}_p$) represents the permittivity (or permeability) tensor of the core by $p = c$ and/or the shell by

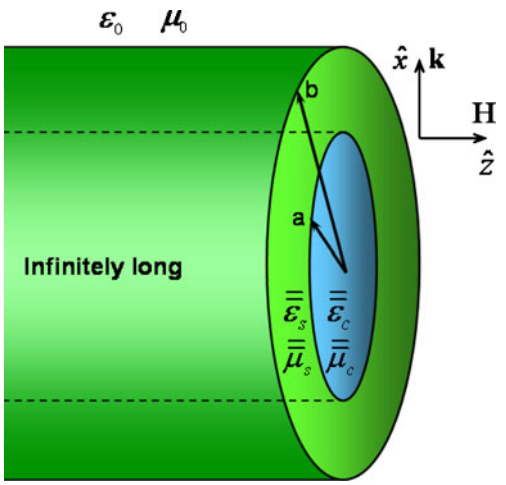


**Fig. 1** Geometry of the scattering of a plane wave by a coated cylinder with permittivity and permeability of cylindrically anisotropic tensors. The incident wave propagates along $x$-axis, and the magnetic field is along $z$-axis

$p = s$. If the anisotropic tensors defined in cylindrical coordinate in this paper is transformed into $(x, y, z)$ coordinate, the material itself will become angle and position dependent which makes the methods in [29] for isotropic cases and [19] for anisotropic cases under rectangular coordinate inapplicable.

In Fig. 1, the incident magnetic field with unit amplitude can be written as $H_z = e^{ik_0 x - i\omega t}$, where $k_0 = \omega\sqrt{\varepsilon_0\mu_0}$. In what follows, $e^{-i\omega t}$ will be omitted. In this connection, Maxwell equations in the core and shell are written as,

$$\nabla \times \mathbf{H} = -i\omega\bar{\bar{\varepsilon}} \times \mathbf{E} \tag{2a}$$

$$\nabla \times \mathbf{E} = i\omega\bar{\bar{\mu}} \times \mathbf{H}. \tag{2b}$$

In cylindrical coordinates, Eq. 2 can be decomposed into

$$i\omega\mu_{pr}H_r = \frac{1}{r}\frac{\partial E_z}{\partial\theta} - \frac{\partial E_\theta}{\partial z} \tag{3a}$$

$$i\omega\mu_{p\theta}H_\theta = \frac{\partial E_r}{\partial z} - \frac{\partial E_z}{\partial r} \tag{3b}$$

$$i\omega\mu_{pz}H_z = \frac{1}{r}\frac{\partial(rE_\theta)}{\partial r} - \frac{1}{r}\frac{\partial E_r}{\partial\theta} \tag{3c}$$

$$-i\omega\varepsilon_{pz}E_z = \frac{1}{r}\frac{\partial(rH_\theta)}{\partial r} - \frac{1}{r}\frac{\partial H_r}{\partial\theta} \tag{3d}$$

$$-i\omega\varepsilon_{pr}E_r = \frac{1}{r}\frac{\partial H_z}{\partial\theta} - \frac{\partial H_\theta}{\partial z} \tag{3e}$$

$$-i\omega\varepsilon_{p\theta}E_\theta = \frac{\partial H_r}{\partial z} - \frac{\partial H_z}{\partial r}. \tag{3f}$$

After some algebraic manipulations, we can obtain the governing equation of $H_z$

$$\frac{1}{\varepsilon_{p\theta}}\frac{\partial}{\partial r}\left(r\frac{\partial H_z}{\partial r}\right) + \frac{1}{r\varepsilon_{pr}}\frac{\partial^2 H_z}{\partial\theta^2} + \omega^2\mu_{pz}rH_z = 0. \tag{4}$$

Inserting the solution in the form of $H_z = \Psi(r)\Theta(\theta)$ and introducing a separation term $m^2$, one obtains the ordinary differential equation for $\Psi(r)$

$$r^2\frac{d^2\Psi(r)}{dr^2} + r\frac{d\Psi(r)}{dr} + \left(\omega^2\varepsilon_{p\theta}\mu_{pz}r^2 - \frac{m^2}{\varepsilon_{pr}/\varepsilon_{p\theta}}\right)\Psi(r) = 0. \tag{5}$$

For the part $\Theta(\theta)$, we have the form $e^{im\theta}$. The general solution to Eq. 5 is $AJ_{pm}(k_p r) + BN_{pm}(k_p r)$, where $J_{pm}$ and $N_{pm}$ respectively denote the $m$th-order Bessel and Neumann functions with the argument of $k_p r$, $k_p^2 = \omega^2\varepsilon_{p\theta}\mu_{pz}$, and $(pm)^2 = \frac{m^2}{(\varepsilon_{pr}/\varepsilon_{p\theta})}$. Note that if it is an isotropic case (i.e., $\varepsilon_{pr} = \varepsilon_{p\theta}$), $pm$ reduces to be an integer.

In order to match the boundary conditions at cylindrical interfaces, the incident magnetic field can be expanded as follows,

$$H_z^{inc} = e^{ik_0 x} = e^{ik_0 r\cos\theta} = \sum_{m=-\infty}^{+\infty} i^m J_m(k_0 r)e^{im\theta}. \tag{6}$$

The total magnetic field in each region can thus be formulated

$$H_z = \sum_{m=-\infty}^{+\infty} A_m J_{cm}(k_c r)e^{im\theta}, \quad r < a, \tag{7a}$$

$$H_z = \sum_{m=-\infty}^{+\infty} i^m[B_m J_{sm}(k_s r) + C_m N_{sm}(k_s r)]e^{im\theta}, \quad a < r < b, \tag{7b}$$

$$H_z = \sum_{m=-\infty}^{+\infty} i^m[J_m(k_0 r) + D_m H_m^{(1)}(k_0 r)]e^{im\theta}, \quad r > b, \tag{7c}$$

where $A_m$, $B_m$, $C_m$, and $D_m$ are the unknown coefficients to be determined and $H_m^{(1)}$ represents the $m$th-order Hankel function of the first kind.

Applying the boundary conditions of $E_\theta$ and $H_z$ being continuous at $r = a$ and $r = b$, we can derive the scattering coefficient $D_m$ to compute the farfield pattern

$$D_m = \frac{\begin{vmatrix} J_{cm}(k_c a) & -J_{sm}(k_s a) & -N_{sm}(k_s a) & 0 \\ \frac{\varepsilon_{s\theta}}{\varepsilon_{c\theta}}k_c J'_{cm}(k_c a) & -k_s J'_{sm}(k_s a) & -k_s N'_{sm}(k_s a) & 0 \\ 0 & J_{sm}(k_s b) & N_{sm}(k_s b) & J_m(k_0 b) \\ 0 & \frac{\varepsilon_0}{\varepsilon_{s\theta}}k_s J'_{sm}(k_s b) & \frac{\varepsilon_0}{\varepsilon_{s\theta}}k_s N'_{sm}(k_s b) & k_0 J'_m(k_0 b) \end{vmatrix}}{\begin{vmatrix} J_{cm}(k_c a) & -J_{sm}(k_s a) & -N_{sm}(k_s a) & 0 \\ \frac{\varepsilon_{s\theta}}{\varepsilon_{c\theta}}k_c J'_{cm}(k_c a) & -k_s J'_{sm}(k_s a) & -k_s N'_{sm}(k_s a) & 0 \\ 0 & J_{sm}(k_s b) & N_{sm}(k_s b) & -H_m^{(1)}(k_0 b) \\ 0 & \frac{\varepsilon_0}{\varepsilon_{s\theta}}k_s J'_{sm}(k_s b) & \frac{\varepsilon_0}{\varepsilon_{s\theta}}k_s N'_{sm}(k_s b) & -k_0 H'^{(1)}_m(k_0 b) \end{vmatrix}}, \tag{8}$$

where the prime denotes the derivative with respect to the argument. Note that other coefficients can also be solved simultaneously, and hence, the electric and magnetic fields in each region are obtained. The scattering problem for the TE case can be solved in a similar way and the corresponding scattering coefficients can be obtained by the duality of $\varepsilon \to \mu$ and $\mu \to \varepsilon$.

Scattering and extinction efficiencies are expressed through scattering amplitudes [29],

$$Q_{\text{sca}} = \frac{2}{k_0 b} \sum_{m=-\infty}^{\infty} |D_m|^2 \quad \text{and}$$

$$Q_{\text{ext}} = \frac{2}{k_0 b} \sum_{m=-\infty}^{\infty} \text{Re}(D_m). \tag{9}$$

## Effective medium theory in long wavelength limit

In this section, we present the formulation of our effective medium theory for the coated cylinders in the long wavelength limit, i.e., $k_0 b \ll 1$ and $k_s b \ll 1$. As a result, the higher-order moments proportional to $(k_i b)^{2l+1}$ $(i = o, c, s)$ are expected to be negligible and the effective scattering width of the coated cylinder is dominated by $m = 0$ and $m = 1$ terms [30, 31]. Thus, we set the conditions for an effective medium as $D_0 = 0$ and $D_1 = 0$ [30], corresponding to

$$\begin{vmatrix} J_0(k_c a) & -J_0(k_s a) & -N_0(k_s a) & 0 \\ \frac{\varepsilon_{s\theta}}{\varepsilon_{c\theta}} k_c J_0'(k_c a) & -k_s J_0'(k_s a) & -k_s N_0'(k_s a) & 0 \\ 0 & J_0(k_s b) & N_0(k_s b) & J_0(k_0 b) \\ 0 & \frac{\varepsilon_0}{\varepsilon_{s\theta}} k_s J_0'(k_s b) & \frac{\varepsilon_0}{\varepsilon_{s\theta}} k_s N_0'(k_s b) & k_0 J_0'(k_0 b) \end{vmatrix} = 0, \tag{10}$$

and

$$\begin{vmatrix} J_{c1}(k_c a) & -J_{s1}(k_s a) & -N_{s1}(k_s a) & 0 \\ \frac{\varepsilon_{s\theta}}{\varepsilon_{c\theta}} k_c J_{c1}'(k_c a) & -k_s J_{s1}'(k_s a) & -k_s N_{s1}'(k_s a) & 0 \\ 0 & J_{s1}(k_s b) & N_{s1}(k_s b) & J_1(k_0 b) \\ 0 & \frac{\varepsilon_0}{\varepsilon_{s\theta}} k_s J_{s1}'(k_s b) & \frac{\varepsilon_0}{\varepsilon_{s\theta}} k_s N_{s1}'(k_s b) & k_0 J_1'(k_0 b) \end{vmatrix} = 0, \tag{11}$$

where the subscripts $s1 = \sqrt{\varepsilon_{s\theta}/\varepsilon_{sr}}$ and $c1 = \sqrt{\varepsilon_{c\theta}/\varepsilon_{cr}}$. In the limit of $k_0 b \ll 1$ and $k_s b \ll 1$, we can use the following approximations $J_0(x) \cong 1$, $N_0(x) \cong \frac{2}{\pi} \ln(x/2)$, $J_0'(x) \cong -x/2$, $N_0'(x) \cong \frac{2}{\pi x}$, $J_1(x) \cong \frac{x}{2}$, $J_1'(x) \cong \frac{1}{2}$, $J_\nu'(x) \cong \frac{\nu J_\nu}{x}$, and $N_\nu'(x) \cong -\frac{\nu N_\nu}{x}$ [32]. Substituting these approximations into Eqs. 10 and 11 and replacing $\varepsilon_0$, $\mu_0$ by $\varepsilon_{\text{eff}}$, $\mu_{\text{eff}}$, respectively, one can obtain

$$\mu_{\text{eff}} = \mu_{sz}\left(1 - \frac{a^2}{b^2}\right) + \frac{a^2}{b^2}\mu_{cz}, \tag{12}$$

and

$$\varepsilon_{\text{eff}} = \frac{\varepsilon_{s\theta}[(c1 \times \varepsilon_{s\theta} + s1 \times \varepsilon_{c\theta}) - (\frac{a}{b})^{2 \times s1}(c1 \times \varepsilon_{s\theta} - s1 \times \varepsilon_{c\theta})]}{s1[(c1 \times \varepsilon_{s\theta} + s1 \times \varepsilon_{c\theta}) + (\frac{a}{b})^{2 \times s1}(c1 \times \varepsilon_{s\theta} - s1 \times \varepsilon_{c\theta})]}. \tag{13}$$

It is evident that, in the long wavelength limit, the electric and magnetic fields are decoupled. For an isotropic case $\varepsilon_{pr} = \varepsilon_{p\theta}$ $(p = c,\ s)$, they reduce to the results in [30]. As a consequence, the coated anisotropic cylinder in the long wavelength limit can be viewed as an effective homogeneous cylinder, and the scattering efficiency is expressed in a simpler form as follows,

$$Q_s = \pi^5 \left(\frac{b}{\lambda_0}\right)^3 \left(\left|\frac{\mu_0 - \mu_{\text{eff}}}{\mu_0}\right|^2 + 2\left|\frac{\varepsilon_0 - \varepsilon_{\text{eff}}}{\varepsilon_0 + \varepsilon_{\text{eff}}}\right|^2\right). \tag{14}$$

Furthermore, the invisibility condition implies that $\varepsilon_{\text{eff}}$ and $\mu_{\text{eff}}$ in Eqs. 12 and 13 should be identical to the parameters of the host medium, i.e., $\varepsilon_0$ and $\mu_0$. Thus, the relation between core–shell ratio and the anisotropic parameters in the core and the shell can be drawn

$$\frac{a}{b} = \sqrt{\frac{\mu_{sz} - \mu_0}{\mu_{sz} - \mu_{cz}}}, \quad \text{purely magnetic} \tag{15}$$

$$\frac{a}{b} = \left[\frac{(c1 \times \varepsilon_{s\theta} + s1 \times \varepsilon_{c\theta})(\varepsilon_{s\theta} - \varepsilon_0 \times s1)}{(c1 \times \varepsilon_{s\theta} - s1 \times \varepsilon_{c\theta})(\varepsilon_{s\theta} + \varepsilon_0 \times s1)}\right]^{1/(2s1)}, \quad \text{purely nonmagnetic.} \tag{16}$$

In fact, the invisibility conditions above possess a physical constraint, i.e., $0 \le a/b \le 1$ according to the set-up in Fig. 1, which implies that, given a certain set of anisotropic parameters for the shell and core, there may be no invisibility no matter how the core–shell ratio is tuned. It is also worth noting that if the coated cylinder is isotropic, Eqs. 15 and 16, respectively, become

$$\frac{a}{b} = \sqrt{\frac{\mu_s - \mu_0}{\mu_s - \mu_c}}, \tag{17}$$

$$\frac{a}{b} = \left[\frac{(\varepsilon_s + \varepsilon_c)(\varepsilon_s - \varepsilon_0)}{(\varepsilon_s - \varepsilon_c)(\varepsilon_s + \varepsilon_0)}\right]^{1/2}, \tag{18}$$

which are in accordance with the results in [13].

## Numerical results

Based on our theoretical results, we provide numerical calculations of the scattering efficiencies under different cylindrical anisotropies and physical insights into the invisibility phenomena. The anisotropy's role upon achieving transparency has actually been translated into the role of "$a/b$" (the radius ratio) corresponding to the critical scattering reduction, once the anisotropic parameters are all specified. One can search for a core–shell ratio "$a/b$" in Eq. 9 where invisibility can be pronounced . Vice versa, if "$a/b$" is given, we can find an anisotropy to get the invisibility.

Figure 2 shows the full-wave scattering efficiency of a plasmonic cylinder coated with dielectric anisotropic shell versus the core–shell ratio $a/b$ at different sizes. First, for small coated cylinder, the long wavelength limit is valid, and hence, one can resort to effective medium theory. In this connection, we discuss the effective permittivity (effective permeability equals $mu_0$ because of nonmagnetic components) in Fig. 2a. We find that, for certain radius ratios $a/b$, the effective permittivity equals $\varepsilon_0$ and the scattering cross section of the coated cylinder is almost zero correspondingly (see the dips in Fig. 2b). As a consequence, the coated cylinder is invisible or transparent. On the contrary, when the effective permittivity equals $-\varepsilon_0$ in Fig. 2a, the surface plasmon resonance takes place and strong scattering cross section is obtained (see the corresponding peaks in Fig. 2b). Then, we calculate the scattering efficiency for larger objects, which are shown in Fig. 2c, d. In this situation, the long wavelength limit is not valid, and the effective medium model cannot be used. In fact, with the object's size being increased, the scattering efficiency can still be reduced significantly (see the dotted lines in Fig. 2c, d) at the certain radius ratio (we call "near-zero scattering" ratio), though these values are larger than those within the long wavelength limit.

Of particular interest is that significant reduction arises if we tune the value of $\varepsilon_{s\theta}$ in the shell. In Fig. 2c, with decreasing $\varepsilon_{s\theta}$ (i.e., be reduced to $2.5\varepsilon_0$), the scattering efficiency can be reduced considerably, and thus, the transparency or nearly "invisible" is attained for large objects. Figure 2d has verified this tendency at an even larger size. In other words, through adjusting the dielectric anisotropy of the shell, it is helpful for us to realize much lower scattering cross section and better electromagnetic invisibility. Moreover, the near-zero scattering radius ratio can be tuned at the same time. We note that a resonant peak is also presented in Fig. 2, in the long wavelength limit (or for small size), and the maximum of scattering is due to the resonance of $D_{\pm 1}^{\mathrm{TM}}$. In comparison with the small objects, the additional small peaks in Fig. 2c, d result from the contributions of $D_{\pm 2}^{\mathrm{TM}}$ because the higher terms of the scattering coefficient cannot be neglected due to the increasing size of the objects.

To give more insights into the effects of anisotropy upon the invisibility performance, total scattering cross

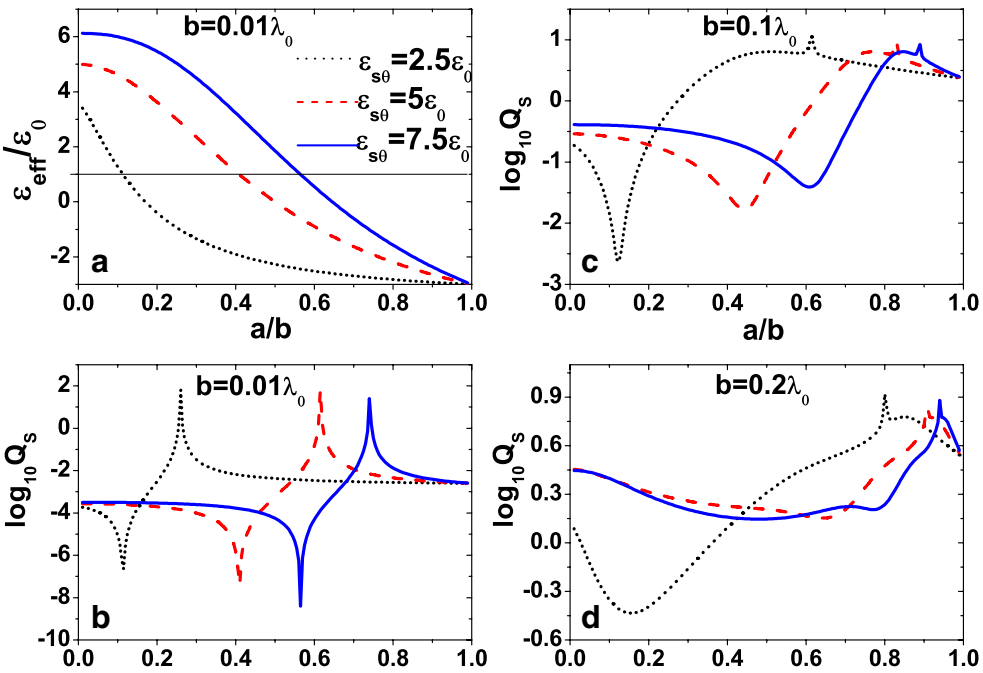


**Fig. 2** **a** The effective permittivity $\varepsilon_{\mathrm{eff}}$ of the coated cylinder versus core–shell ratio for different $\varepsilon_{s\theta}$ when $b = 0.01\lambda_0$. **b–d** The scattering efficiency versus core–shell ratio for different $\varepsilon_{s\theta}$ and different values of $b$. $\varepsilon_{s\theta} = 2.5\varepsilon_0$ (*black dotted line*); $\varepsilon_{s\theta} = 5\varepsilon_0$ (*red dashed line*); $\varepsilon_{s\theta} = 7.5\varepsilon_0$ (*blue solid line*). Other parameters are $\varepsilon_{cr} = \varepsilon_{c\theta} = -3\varepsilon_0$, $\varepsilon_{sr} = 5\varepsilon_0$, $\mu_{sz} = \mu_{cz} = \mu_0$

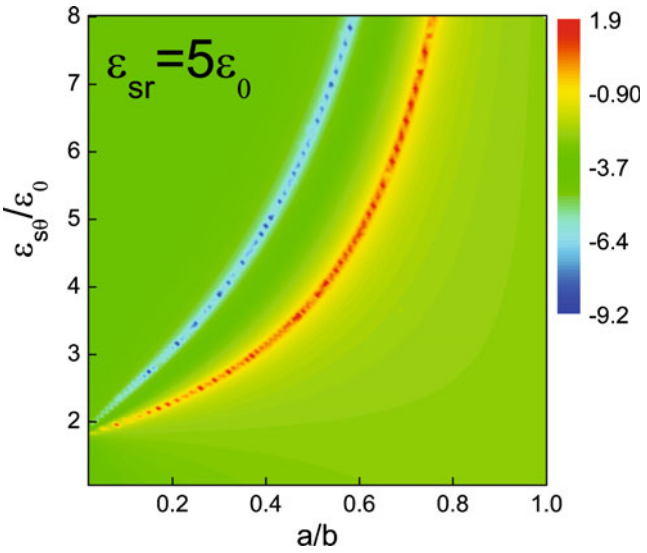


**Fig. 3** The contour plot of the total scattering cross section $\log_{10} Q_s$ at different $\varepsilon_{s\theta}$ (i.e., different anisotropies) when $b = 0.01\lambda_0$ and $\varepsilon_{cr} = \varepsilon_{c\theta} = -3\varepsilon_0, \quad \mu_{sz} = \mu_{cz} = \mu_0$

section corresponding to the anisotropy as well as the core–shell ratio is studied in Fig. 3. The blue string indicates the suitable anisotropy and associated core–shell ratio with which the total scattering can be drastically reduced. On the other hand, the other string in red denotes the anisotropy and core–shell ratio needed for enhanced scattering, which is not the focus of the current paper.

Next, we consider a coated cylinder with cylindrically anisotropic core but isotropic shell as shown in Fig. 4. Again, for a small coated cylinder, it is evident that the minimum of the scattering cross section takes place at the core–shell radius ratio determined by the condition $\varepsilon_{\text{eff}} = \varepsilon_0$. Hence, the results based on the full-wave theory should be in accordance with those from effective medium theory. We can observed from Fig. 4b–d that the isotropic core results in the smallest scattering efficiency, i.e., better electromagnetic invisibility (e.g., red dashed curves in Fig. 4 representing isotropic cores in each case). This fact is further proved for larger sizes (see Fig. 4c, d), and even for either plasmonic core with dielectric shell (see Fig. 4c) or dielectric core with plasmonic shell (see Fig. 4d). It reveals that, in the core–shell system incorporating cylindrical anisotropy, the isotropy in the core is a better choice to minimize the scattering width, resulting in "good" invisibility.

It is known that, for large coated objects, multipolar terms contribute to the scattering cross section, and the

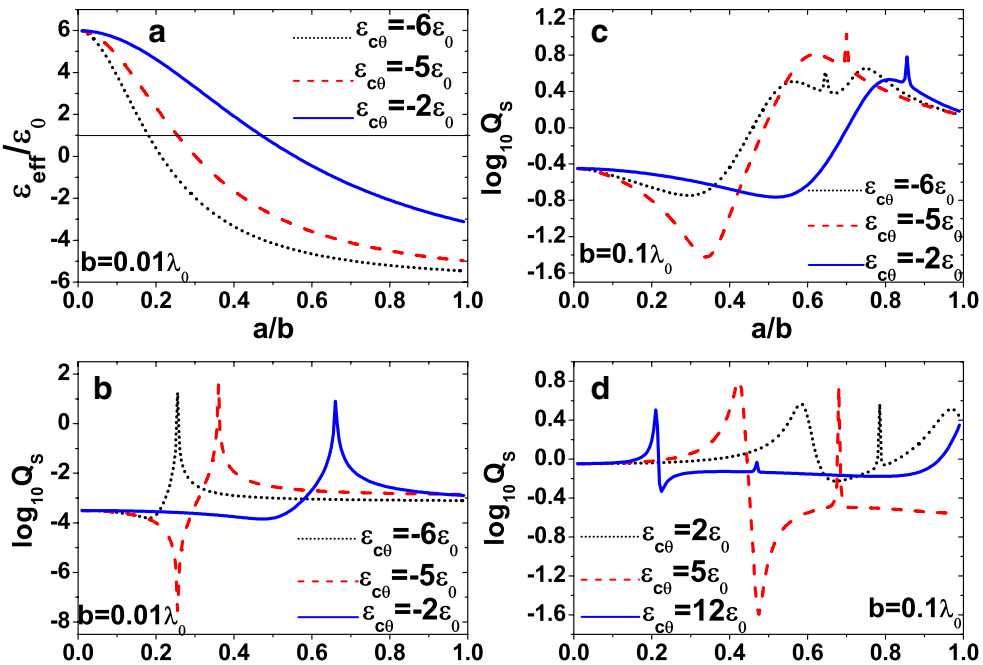


**Fig. 4** **a** The effective permittivity $\varepsilon_{\text{eff}}$ of the coated cylinder versus core–shell ratio for different $\varepsilon_{c\theta}$ when $b = 0.01\lambda_0$. **b–c** The scattering efficiency versus core–shell ratio for different values of $b$ and different $\varepsilon_{c\theta}$. The values of $\varepsilon_{c\theta}$ in **a–c** are: $\varepsilon_{c\theta} = -6\varepsilon_0$ (*black dotted line*); $\varepsilon_{c\theta} = -5\varepsilon_0$ (*red dashed line*); $\varepsilon_{c\theta} = -2\varepsilon_0$ (*blue solid line*), while other parameters in **a–c** are $\varepsilon_{cr} = -5\varepsilon_0, \quad \varepsilon_{s\theta} = \varepsilon_{sr} = 6\varepsilon_0, \quad \mu_{sz} = \mu_{cz} = \mu_0$. **d** The full-wave scattering efficiency versus core–shell ratio for $b = 0.1\lambda_0$ with $\varepsilon_{c\theta} = 2\varepsilon_0$ (*black dotted line*), $\varepsilon_{c\theta} = 5\varepsilon_0$ (*red dashed line*), and $\varepsilon_{c\theta} = 12\varepsilon_0$ (*blue solid line*), while the other parameters are $\varepsilon_{cr} = 5\varepsilon_0, \quad \varepsilon_{s\theta} = \varepsilon_{sr} = -10\varepsilon_0, \quad \mu_{sz} = \mu_{cz} = \mu_0$

coated cylinder is visible for almost all the radius ratio (see Fig. 5). In order to make the coated cylinder transparent or at least less visible, one can further adjust the magnetic anisotropy to reduce the scattering cross section. From Fig. 5, we can conclude that the invisibility effectiveness of large objects can be greatly improved through suitable adjustment of both the dielectric and magnetic anisotropy and the scattering efficiency can be reduced for nearly one order in magnitude.

If the size is sufficiently small, the core–shell ratio determined by the cloaking condition definitely results in better invisibility performance. In order to demonstrate the invisibility performance for a large size $b = 0.2\lambda_0$ improved by the adjustment of the magnetodielectric anisotropy, we present the patterns of magnetic field in the $xy$ plane, calculated by finite-element solver of the Comsol Multiphysics. In Fig. 6a, for the isotropic case (the same parameters as the red dashed line in Fig. 2d), there exists noticeable perturbation caused by the scattered field. Comparing Fig. 6b with a, one can see that the perturbation is reduced through adjusting the anisotropic permittivity of the shell. If we take the permeability into account and properly tune its value, the near "invisibility" could be achieved for even relatively larger objects. In Fig. 6c, the incident wave is almost unaltered outside the shelled cylinder, as if there was no scatterer. The specific core–shell ratios chosen in Fig. 6 are based on the given material parameters and obtained in numerical calculation for the lowest scattering efficiency correspondingly instead of theoretical effective medium theory (due to the size constraint). It should be mentioned that the transparency mechanism in this paper is different from the ideal cloak proposed by Pendry [1] via spatial compression, where there is no EM field in the core cylinder. Here, the coated cylinder is penetrable.

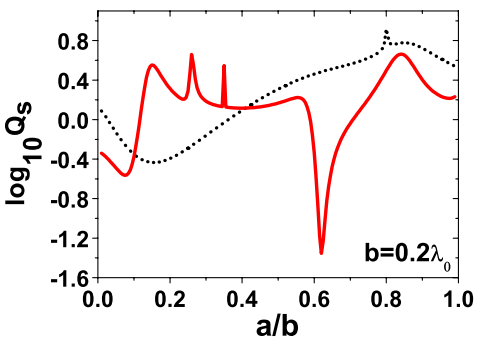


**Fig. 5** The full-wave scattering efficiency versus core–shell ratio for $b = 0.2\lambda_0$. Parameters for the *black dotted curve*: $\varepsilon_{c\theta} = \varepsilon_{cr} = -3\varepsilon_0$, $\varepsilon_{s\theta} = 2.5\varepsilon_0$, $\varepsilon_{sr} = 5\varepsilon_0$, $\mu_{sz} = \mu_{cz} = \mu_0$. Parameters for the *red solid curve*: $\varepsilon_{c\theta} = \varepsilon_{cr} = -3\varepsilon_0$, $\varepsilon_{s\theta} = 2.5\varepsilon_0$, $\varepsilon_{sr} = 5\varepsilon_0$, $\mu_{sz} = 0.5\mu_0$, $\mu_{cz} = -7\mu_0$

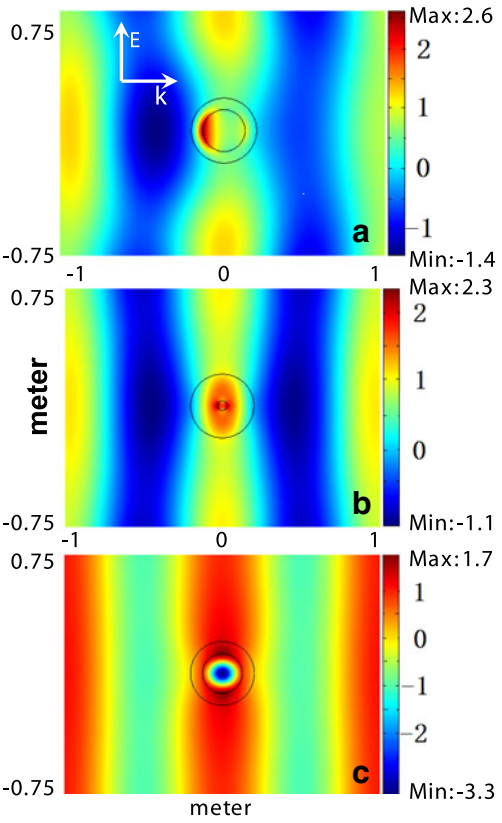


**Fig. 6** Snapshots of the real part of total $H_z$ fields distribution in the $xy$ plane around the coated cylinder with outer radius $b = 0.2\lambda_0$ at 0.3GHz. **a** Parameters are: $\varepsilon_{c\theta} = \varepsilon_{cr} = -3\varepsilon_0$, $\varepsilon_{s\theta} = 5\varepsilon_0$, $\varepsilon_{sr} = 5\varepsilon_0$, $\mu_{sz} = \mu_{cz} = \mu_0$, $a = 0.645b$. **b** Parameters are: $\varepsilon_{c\theta} = \varepsilon_{cr} = -3\varepsilon_0$, $\varepsilon_{s\theta} = 2.5\varepsilon_0$, $\varepsilon_{sr} = 5\varepsilon_0$, $\mu_{sz} = \mu_{cz} = \mu_0$, $a = 0.155b$. **c** Parameters are: $\varepsilon_{c\theta} = \varepsilon_{cr} = -3\varepsilon_0$, $\varepsilon_{s\theta} = 2.5\varepsilon_0$, $\varepsilon_{sr} = 5\varepsilon_0$, $\mu_{sz} = 0.5\mu_0$, $\mu_{cz} = -7\mu_0$, $a = 0.62b$

## Conclusion

In summary, we have demonstrated the full-wave scattering theory by magnetodielectric anisotropic coated cylinder of infinite length normally illuminated by a TM-polarized plane wave. The effective permittivity and permeability of the anisotropic coated cylinder have also been derived in long wavelength limit. The nonscattering radius ratio obtained from the full-wave theory for small objects can be well described within the effective medium theory. Numerical results have shown that the effective scattering width $c_{\text{sca}} = 2b\,Q_{\text{sca}}$ can be significantly reduced by adjusting the anisotropic permittivity of the shell, so as to achieve better transparency. However, it is found that tuning the core anisotropy is not able to improve the efficiency of transparency. Furthermore, we could further improve the invisibility performance of the cylindrical objects by the adjustment of both electric and magnetic anisotropies.

Although we have only considered the 2D case and losses materials, our research may be useful for the design of low-observability cylindrical targets. Based on the above investigation, we may extend our investigation to more general situations, such as obliquely incidence with arbitrary polarization, and finite-long cylinders. We could scale well toward the research of making multiple cylindrical objects "invisible".

**Acknowledgements** This work was supported by the National Natural Science Foundation of China under Grant No. 10674098, the National Basic Research Program under Grant No. 2004CB719801, the Key Project in Science and Technology Innovation Cultivation Program of Soochow University, and the Natural Science of Jiangsu Province under Grant No. BK2007046.

## References

1. Pendry JB, Schurig D, Smith DR (2006) Controlling electromagnetic fields. Science 312:1780–1782
2. Leonhardt U (2006) Optical conformal mapping. Science 312:1777–1780
3. Cummer SA, Popa B-I, Schurig D, Smith DR, Pendry JB (2006) Full-wave simulations of electromagnetic cloaking structures. Phys Rev E 74(3):036621
4. Zhao Y, Argyropoulos C, Hao Y (2008) Full-wave finite-difference time-domain simulation of electromagnetic cloaking structures. Opt Express 16(9):6717–6730
5. Schurig D, Mock JJ, Justice BJ, Cummer SA, Pendry JB, Starr AF, Smith DR (2006) Metamaterial electromagnetic cloak at microwave frequencies. Science 314:977–980
6. Cai W, Chettiar UK, Kildishev AV, Shalaev VM (2007) Optical cloaking with metamaterials. Nat Photonics 1:224–227
7. Ruan Z, Yan M, Neff CW, Qiu M (2007) Ideal cylindrical cloak: perfect but sensitive to tiny perturbations. Phys Rev Lett 99(11):113903
8. Chen HS, Wu BI, Zhang BL, Kong JA (2007) Electromagnetic wave interactions with a metamaterial cloak. Phys Rev Lett 99(6):063903
9. Jiang W, Cui T, Yang X, Cheng Q, Liu R, Smith D (2008) Invisibility cloak without singularity. Appl Phys Lett 93(19):194102
10. Kwon DH, Werner DH (2008) Two-dimensional eccentric electromagnetic cloaks. Appl Phys Lett 92(1):013505
11. Rahm M, Schurig D, Roberts DA, Cummer SA, Smith DR, Pendry JB (2008) Design of electromagnetic cloaks and concentrators using form-invariant coordinate transformations of Maxwell's equations. Photon Nanostruct Fundam Applic 6(1):87–95
12. Ma H, Qu S, Xu Z, Wang J (2008) Numerical method for designing approximate cloaks with arbitrary shapes. Phys Rev E 78(3):036608
13. Alú A, Engheta N (2005) Achieving transparency with plasmonic and metamaterial coatings. Phys Rev E 72(1):016623
14. Silveirinha MG, Alú A, Engheta, N (2007) Parallel-plate metamaterials for cloaking structures. Phys Rev E 75(3):036603
15. Gao L, Fung TH, Yu KW, Qiu CW (2008) Electromagnetic transparency by coated spheres with radial anisotropy. Phys Rev E 78(4):046609
16. Qiu CW, Hu L, Xu X, Feng Y (2009) Spherical cloaking with homogeneous isotropic multilayered structures. Phys Rev E 79(4):047602
17. Yan M, Ruan Z, Qiu M (2007) Scattering characteristics of simplified cylindrical invisibility cloaks. Opt Express 15(26):17772–17782
18. Luo Y, Zhang J, Chen H, Xi S, Wu B-I (2008) Cylindrical cloak with axial permittivity/permeability spatially invariant. Appl Phys Lett 93:033504
19. Uslenghi PLE, Graglia RD (1984) Electromagnetic scattering from anisotropic materials. Part I: general theory IEEE Trans Antennas Propag 32(8):867–869
20. Graglia RD, Uslenghi PLE (1987) Electromagnetic scattering from anisotropic materials, part II: computer code and numerical results in two dimensions. IEEE Trans Antennas Propag 35(2):225–232
21. Monzon, JC, Damaskos NJ (1986) Two-dimensional scattering by a homogeneous anisotropic rod. IEEE Trans Antennas Propag 34(10):1243–1249
22. Beker B, Umashankar KR, Taflove A (1989) Numerical analysis and validation of the combined field surface integral equations for electromagnetic scattering by arbitrary shaped two-dimensional anisotropic objects. IEEE Trans Antennas Propagat 37(12):1573–1581
23. Tai CT (1994) Dyadic Green's functions in electromagnetic theory, 2nd edn. IEEE, Piscataway
24. Uzunoglu NK, Gottis PG, Fikioris JG (1995) Excitation of electromagnetic waves in a gyroelectric cylinder. IEEE Trans Antennas Propag 33(1):90–99
25. Qiu CW, Li LW, Yao H, Zouhdi S (2006) Properties of Faraday chiral media: Green dyadics and negative refraction. Phys Rev B 74(11):115110
26. Qiu CW, Zouhdi S, Razek A (2007) Modified spherical wave functions with anisotropy ratio: application to the analysis of scattering by multilayered anisotropic shells. IEEE Trans Antennas Propag 55(12):3515–3523
27. Mitamura K, Imae T (2009) Functionalization of gold nanorods toward their applications. Plasmonics 4(1): 23–30
28. Yong K-T, Swihart MT, Ding H, Prasad PN (2009) Preparation of gold nanoparticles and their applications in anisotropic nanoparticle synthesis and bioimaging. Plasmonics 4(2):79–93
29. van de Hulst HC (1957) Light scattering by small particles. Wiley, New York
30. Wu Y, Li, JS, Zhang ZQ, Chan CT (2006) Effective medium theory for magnetodielectric composites: beyond the long-wavelength limit. Phys Rev B 74(8):085111
31. Luk'yanchuk BS, Ternovsky V (2006) Light scattering by a thin wire with a surface-plasmon resonance: bifurcations of the Poynting vector field. Phys Rev B 73(23):235432
32. Jackson JD (1999) Classical electrodynamics, 3rd edn. Wiley, New York